Exchange interactions in two-dimensional materials of $MnBi_2Te_4$-type

Donya Mazhjoo[a], Gustav Bihlmayer[a], and Stefan Blügel[a]

[a]Peter Grünberg Institut and Institute for Advanced Simulation, Forschungszentrum Jülich and JARA, 52425 Jülich, Germany

ABSTRACT

Septuple layers of $MnBi_2Te_4$ type are important building blocks of magnetic topological insulators and semimetals but also examples of two-dimensional magnetic materials with critical temperatures up to a few tens of Kelvin. Using density functional theory (DFT) we study the exchange interactions in $MnBi_2Te_4$, $MnBi_2Se_4$, and $MnSb_2Te_4$ films to highlight the importance of higher-order terms and the contributions of relativistic anisotropic interactions. We also discuss the possibility to induce Dzyaloshinskii-Moriya interaction by gating with an external electric field.

Keywords: 2D magnetic materials, exchange interactions, density functional theory

1. INTRODUCTION

Due to their novel properties and the high variability allowed by their stacking, two-dimensional materials have attracted considerable interest in the last decade.[1] For spintronic applications, magnetic materials are highly desirable and indeed several examples have been intensively studied up to now. From the point of view of magnetic interactions they include Heisenberg-like systems, e.g. $Cr_2Ge_2Te_6$ where the ordering temperature is tiny in the monolayer regime[2] as well as Ising-like magnets, e.g. CrI_3 with a relatively high ordering temperature of 45 K for the monolayers.[3] Still higher values have been achieved in Fe_3GeTe_2[4] and even room temperature ferromagnetism was found in VSe_2 monolayers.[5] Also intrinsically magnetic topological materials like $MnBi_2Te_4$ have been found that are layer-wise antiferromagnetic (AFM) in the bulk but can be combined with layers of similar topological insulators.[6] Therefore, it is of substantial interest to study the magnetic interactions in materials of this type and see how they are altered by their chemical constitution. Since the classical Heisenberg-type interactions are small[7] and not sufficient to stabilize long range magnetic order it is important to study also higher-order and anisotropic interactions here.[8] After a short presentation of the computational details, we first address non-relativistic interactions, both pair-wise and higher-order terms. Then we study the interactions that result from relativistic effects and conclude with a short discussion.

2. COMPUTATIONAL DETAILS

We performed self-consistent DFT calculations in the generalized gradient approximation (GGA)[9] employing the full-potential linearized augmented planewave method[10] as implemented in the FLEUR code.[11] The experimental unit cell parameters as given in Ref. 12 and listed in table 2 were used for the in-plane lattice constants. The septuple-layer films were relaxed in out-of-plane direction showing a contraction of about 0.4 Å between the outermost layers and an expansion of about 0.5 Å between the second and third layer. The inner layers show expansions < 0.1 Å. The planewave cutoff for the basis functions was set to $K_{\max} = 4.0$ a.u.$^{-1}$. The charge density was expanded up to a cutoff $G_{\max} = 9.4$ a.u.$^{-1}$. We set the muffin-tin radii to $R_{\mathrm{MT}} = 2.50$ a.u., Bi $5d$-states were included ad local orbitals. With a focus on applying DFT+U, we assume $l = 2$, $U = 6.0$ eV and $J = 0.66$ eV for Mn. In the simple unit cell we have used 144 **k**-points in the full Brillouin zone to achieve a well-converged charge density. For the calculation of the magnetocrystalline anisotropy a denser grid with 361 points was used. For the 4×1, 1×4 and 2×2 unit cells, we used $4 \times 14 \times 1$, $7 \times 6 \times 1$ and $7 \times 7 \times 1$ **k**-meshes,

Further author information: (Send correspondence to G.B.)
G.B.: E-mail: g.bihlmayer@fz-juelich.de

respectively. For the calculation of the anisotropic exchange interactions in the 2×1 unit cell a finer $18 \times 12 \times 1$ grid was employed. For the calculations of spiral spin density waves the generalized Bloch theorem was used.[13] In these cases, spin-orbit coupling (SOC) was taken into account using first order perturbation theory.[14]

3. RESULTS

3.1 Heisenberg-type exchange

We start from a classical spin Hamiltonian with spins $\mathbf{S}_i$ containing just two-site interactions, i.e. in general

$$H = \sum_{\langle i,j \rangle} \mathbf{S}_i \underline{J}_{ij} \mathbf{S}_j = \left(\sum_{\langle i,j \rangle}{}' \underline{1} J_{ij} \mathbf{S}_i \cdot \mathbf{S}_j + \sum_i \mathbf{S}_i \underline{K}_{ii} \mathbf{S}_i + \sum_{\langle i,j \rangle}{}' \mathbf{S}_i \underline{J}^s_{ij} \mathbf{S}_j + \sum_{\langle i,j \rangle}{}' \mathbf{S}_i \underline{J}^a_{ij} \mathbf{S}_j \right) \tag{1}$$

where underlined quantities indicate 3×3 matrices and superscripts s and a denote traceless symmetric and antisymmetric matrices. The summations go over unique pairs and the prime in the sum indicates that $i = j$ is excluded. In this notation J_{ij} is the isotropic Heisenberg-type exchange, $\underline{K}_{ii}$ the single-site anisotropy, $\underline{J}^s_{ij}$ the pseudo-dipolar interaction and $\underline{J}^a_{ij}$ the Dzyaloshinskii-Moriya interaction (DMI). All but the first mentioned interaction are of relativistic origin and will be discussed later.

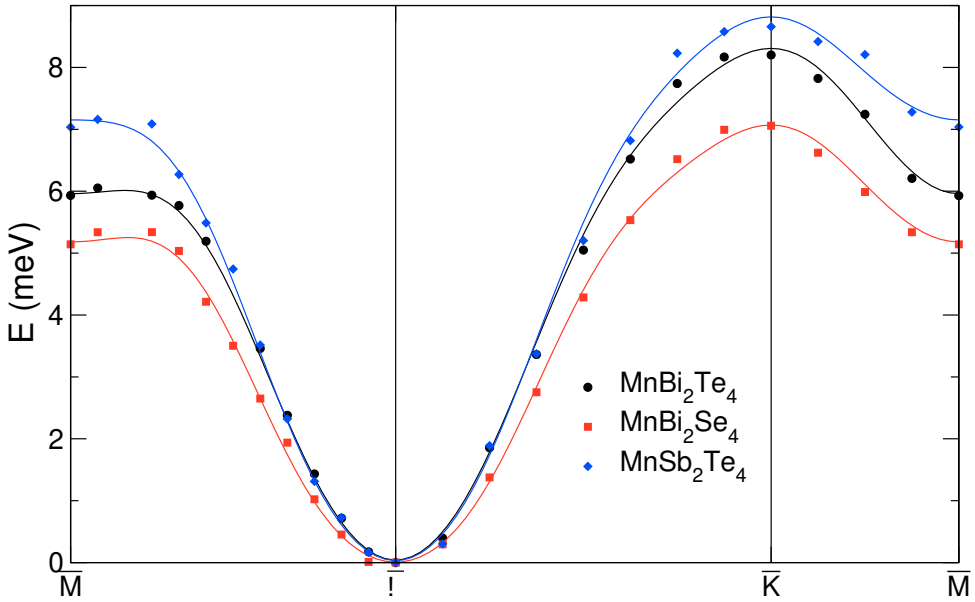

Figure 1. Energy dispersion of spin-spiral states with $\mathbf{q}$-vector along the high symmetry lines $\overline{\mathrm{M\Gamma}}$ and $\overline{\mathrm{\Gamma KM}}$. The data for $MnBi_2Te_4$, $MnBi_2Se_4$, and $MnSb_2Te_4$ are shown with black filled circles, red squares and blue diamonds, respectively. The lines in corresponding colors are fits to the data using a Heisenberg model up to the fifth nearest neighbors.

Since spin-spirals, i.e. states where the magnetization rotates from atom to atom by a fixed angle, are analytical solutions of the classical Heisenberg model, it is convenient to extract the scalar exchange constants from such spin-spiral calculations that can be conveniently performed using the generalized Bloch theorem.[15]

As can be seen from table 1 (and was also predicted for bulk $MnBi_2Te_4$ in Ref. 7), the exchange is dominated by the nearest neighbor interaction. The fact that J_1 favors a ferromagnetic (FM) interaction was analyzed by Li et al.,[16] who related the strength of the FM interaction in $MnBi_2Te_4$ to the position of the unoccupied Bi p-states. A p-band position close to the Fermi level favors FM order, while artificially pushing the band higher up resulted in an AFM ground state. To some extent, this trend can also be observed in the comparison of data shown in table 1 to the densities of states (DOS) plotted in fig. 2: Compared to $MnBi_2Te_4$, the larger band

Table 1. Heisenberg exchange parameters for the first five nearest neighbors obtained by a fit based on the classical Heisenberg model to the spin-spiral energies shown in Fig. 1. The large value of J_3 contains in fact a significant contribution of the nearest-neighbor biquadratic interaction (see subsection 3.2).

Compound	S^2J_1 (meV)	S^2J_2 (meV)	S^2J_3 (meV)	S^2J_4 (meV)	S^2J_5 (meV)
$MnBi_2Te_4$	−1.56	−0.03	−0.35	0.03	0.04
$MnBi_2Se_4$	−1.39	−0.05	−0.26	0.04	0.06
$MnSb_2Te_4$	−1.79	−0.10	−0.21	0.02	0.06

gap of $MnBi_2Se_4$ leads to a higher lying local Bi DOS and a reduced exchange constant $|J_1|$. In contrast, the smaller band gap of $MnSb_2Te_4$ correlates with the larger $|J_1|$ seen in the antimonide. At the same time, the position of the occupied Mn d-states also follows this trend: When they are higher (closer to the Fermi level) $|J_1|$ is decreased while a lower d-band leads to a stronger FM interaction. This trend can also be observed in calculations with different values of the Hubbard-U, where a large U leads to more pronounced ferromagnetism.[8]

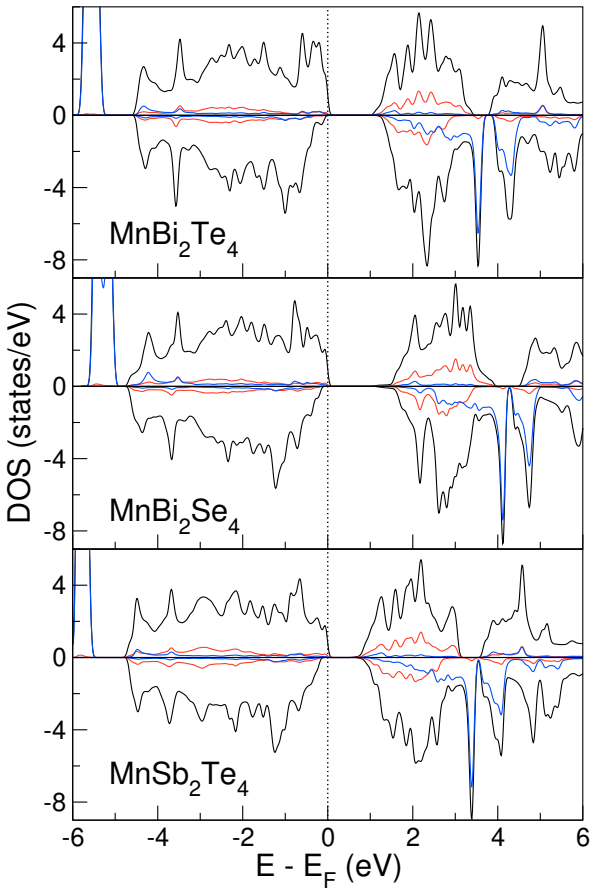

Figure 2. Density of states (DOS) for $MnBi_2Te_4$, $MnBi_2Se_4$, and $MnSb_2Te_4$. The spin-up and spin-down part are shown by positive and negative values, respectively. The total DOS is shown in black, the partial Mn DOS in blue and the Bi/Sb DOS in red.

We conclude here by noting that the above analysis of the exchange couplings, J, was done under the assumption that only 2-spin terms are relevant. In fact, we will see below that this is not so and contributions of higher order interactions are responsible for the apparently large value of J_3.

3.2 Higher-order interactions

Up to now, we considered two-site (or two-spin) interactions but there is no reason to limit the description of the magnetic system to these terms. The next terms appearing in a classical spin model are four-spin interactions, e.g. the biquadratic and the cyclic 4-spin interaction terms

$$H_4 = {\sum_{i,j}}' \mathcal{B}_{ij} (\mathbf{S}_i \cdot \mathbf{S}_j)^2 + {\sum_{i,j,k,l}}' \mathcal{K}_{ijkl} \left[(\mathbf{S}_i \cdot \mathbf{S}_j)(\mathbf{S}_k \cdot \mathbf{S}_l) + (\mathbf{S}_j \cdot \mathbf{S}_k)(\mathbf{S}_l \cdot \mathbf{S}_i) - (\mathbf{S}_i \cdot \mathbf{S}_k)(\mathbf{S}_j \cdot \mathbf{S}_l) \right] . \tag{2}$$

The latter term appears in an analysis of spin 1/2 systems, in systems with higher spins more terms (like the biquadratic one) are possible:[17] Recently, the importance of a 4-spin, 3-site interaction that has the form

$$H_3 = {\sum_{i,j,k}}' \mathcal{Y}_{ijk} \left[(\mathbf{S}_i \cdot \mathbf{S}_j)(\mathbf{S}_j \cdot \mathbf{S}_k) + (\mathbf{S}_j \cdot \mathbf{S}_k)(\mathbf{S}_k \cdot \mathbf{S}_i) + (\mathbf{S}_k \cdot \mathbf{S}_i)(\mathbf{S}_i \cdot \mathbf{S}_j) \right] \tag{3}$$

was demonstrated for ultrathin Fe films on 4*d* substrates.[17,18]

To separate the influence of these higher-order terms from the (usually) larger two-spin contributions, it is convenient to investigate so-called multi-**Q** structures, commensurate magnetic structures that result from a superposition of spin-spiral states (single-**Q**) that preserves the size of the local spins.[19] Since single- and multi-**Q** states are degenerate in the Heisenberg model, the energy difference can be traced back to higher-order interactions.

On the hexagonal lattice, a 3-**Q** state can be formed from the superposition of three row-wise antiferromagnetic states ($\overline{\mathrm{M}}$-point in fig. 1), and – based on DFT calculations – has been proposed to be the ground state for a Mn monolayer on Cu(111).[20] Recently, it was experimentally found for Mn on Re(0001).[21] The energy difference between the 3-**Q** and the 1-**Q** state is (in nearest-neighbor approximation):

$$E_{3\mathbf{Q}(\overline{\mathrm{M}})} - E_{1\mathbf{Q}(\overline{\mathrm{M}})} = -\frac{16}{3} S^4 \left(2\mathcal{K}_1 + \mathcal{B}_1 - \mathcal{Y}_1 \right) . \tag{4}$$

To determine all three constants occurring on the right side of this equation, we need in addition two other multi-**Q** states. Two 2-**Q** structures can be constructed from spin-spirals at $1/2\overline{\Gamma\mathrm{M}}$ and at $3/4\overline{\Gamma\mathrm{K}}$, respectively. These double-**Q** states are collinear double-row wise AFM structures running in orthogonal directions.[22] Also here, an experimental realization was found for a monolayer of Fe on Rh(111).[18] The energy differences are

$$E_{2\mathbf{Q}(\overline{\Gamma\mathrm{M}})} - E_{1\mathbf{Q}(\overline{\Gamma\mathrm{M}})} = -4S^4 \left(2\mathcal{K}_1 - \mathcal{B}_1 - \mathcal{Y}_1 \right) \tag{5}$$

and

$$E_{2\mathbf{Q}(\overline{\Gamma\mathrm{K}})} - E_{1\mathbf{Q}(\overline{\Gamma\mathrm{K}})} = -4S^4 \left(2\mathcal{K}_1 - \mathcal{B}_1 + \mathcal{Y}_1 \right) . \tag{6}$$

The energy differences in eqs. 4, 5 and 6 can be obtained from non-collinear calculations with four magnetic atoms in 2×2, 4×1, and 1×4 unit cells, leading to 2.33 meV, −1.13 meV and −1.18 meV, respectively. Inserting in the equations above gives $S^4\mathcal{K}_1 = -0.04$ meV, $S^4\mathcal{B}_1 = -0.36$ meV, and $S^4\mathcal{Y}_1 = 0.01$ meV. Although these values are small, $S^4\mathcal{B}_1$ is the second biggest term after S^2J_1 and competing with the S^2J_n terms for $n > 1$ in table 1. In fact, as mentioned earlier, the $\mathcal{B}_1$ term also contributes to the spin-spirals shown in fig. 1 and has for the lines $\overline{\mathrm{M}\Gamma}$ and $\overline{\Gamma\mathrm{KM}}$ the same functional form as J_3. Therefore, the large value of J_3 in table 1 is in fact caused by $\mathcal{B}_1$.

3.3 Relativistic effects

3.3.1 Magnetic anisotropy

In two-dimensional magnetic systems long range magnetic order is stabilized by anisotropic interactions that can originate from different sources: dipolar and pseudo-dipolar magnetic interactions or single-site anisotropy. The dipole-dipole interaction is a relativistic two-particle effect not considered in DFT calculations but can be well approximated by a classical dipole sum.[23] We compare out-of-plane ($\perp$) and in-plane ($\parallel$) configurations and list the resulting values $\Delta E_{\mathrm{dip}} = E^{\perp}_{\mathrm{dip}} - E^{\parallel}_{\mathrm{dip}}$ in table 2. As expected for a thin film, they indicate a preference for

in-plane magnetization direction. Moreover, these values are in the same order of magnitude as the single-site or magnetocrystalline anisotropy (MCA), ΔE_{MCA}, that results from spin-orbit interaction. As can be seen, the presence of heavier elements (Bi, Te) leads to larger values of the MCA compared to compounds with lighter (Sb, Se) atoms. The influence of the chalcogen atom, neighboring the magnetic atom, is stronger than that of the pnictogen atom that is in the second nearest layer. In total, these effects result in a negative magnetic anisotropy energy (MAE), i.e. an out-of-plane easy axis, for $MnBi_2Te_4$ and an easy-plane magnetism for $MnBi_2Se_4$. For $MnSb_2Te_4$ the effects almost cancel and the MAE vanishes within the error bars of the calculation.

Table 2. In-plane lattice constant, a, spin magnetic moment, M, dipole-dipole contribution to the magnetic anisotropy, ΔE_{dip}, magnetocrystalline anisotropy, ΔE_{MCA}, and total magnetic anisotropy, ΔE_{MAE}, for the septuple-layer films. Negative (positive) energy values indicate a preference for an out-of-plane (in-plane) easy axis.

Compound	a (Å)	$M(\mu_{\mathrm{B}})$	ΔE_{dip} (meV)	ΔE_{MCA} (meV)	ΔE_{MAE} (meV)
$MnBi_2Te_4$	4.33	4.65	0.118	−0.162	−0.062
$MnBi_2Se_4$	4.07	4.69	0.145	−0.030	0.115
$MnSb_2Te_4$	4.26	4.79	0.132	−0.126	0.006

In situations where the single-site anisotropy is small, anisotropic exchange interactions can make a decisive contribution to the spin-wave gap that stabilizes magnetic order in two dimensions. In the model employed by Torelli et al.,[24] the gap takes the form $\Delta = A(2S-1)+BSN_{\mathrm{nn}}$ where A is the (negative) single-site anisotropy and B is the difference of the elements in the trace of the exchange tensor, $J^{zz} - J^{xx}$ (assuming in-plane anisotropy, $J^{yy} = J^{xx}$). Our calculations for $MnBi_2Te_4$ give $J^{zz} = 1.648$ meV, $J^{yy} = 1.628$ meV, and $J^{xx} = 1.634$ meV, so that $B = 0.017$ meV when we average the in-plane values (a small anisotropy is caused by numerical artifacts from the representation of the exchange correlation potential in our case). These variations are small, but in the order of magnitude of values reported recently.[8] Although the value of B is small, it leads to a significant increase of the Curie temperature: neglecting B results in $T_{\mathrm{C}} = 20.5$ K, while its inclusion leads to $T_{\mathrm{C}} = 23.6$ K when we employ the model of Ref. 24. Note, that the J values above include the isotropic exchange interaction (1.64 meV) that is rather similar to the value obtained without spin-orbit interaction included (1.56 meV).

3.3.2 Dzyaloshinskii-Moriya interaction

Although inversion symmetry excludes the presence of DMI in septuple layers of $MnBi_2Te_4$ type, in reality this inversion symmetry is broken when the layer is deposited on some substrate or embedded in layers of different composition. Therefore, it is of interest to check how these layers respond to symmetry breaking by an electric field. Whether this field is actually applied by some electrode or via the chemical environment is here of secondary importance. In the films of $MnBi_2Te_4$ on Bi_2Te_3 considered in Ref. 6, the presence of Bi_2Te_3 on one and vacuum on the other side, a finite DMI is clearly expected.

To simulate the influence of the electric field we make use of the thin-film geometry[10] of our method and modify the vacuum potential to represent two electrodes of opposite polarity placed about 6 Å above the film surfaces. The electric field is then given by the charges on the electrodes and modified by the dielectric response inside the septuple layer. We applied fields of 3.89 V/nm and 7.79 V/nm that give a reasonable change of the work-function on a free surface. Self-consistent spin-spiral calculations were performed with these changed boundary conditions and spin-orbit effects were included in first order perturbation theory.[14]

From Fig. 3 it is apparent that E_{DMI} is linear in $|\mathbf{q}|$ for long range spin-spirals and we obtain the DMI spiralization from a fit to $E_{\mathrm{DMI}} = \frac{D}{2\pi}|\mathbf{q}| + \mathcal{O}(q^3)$. (For the relation between D and $\underline{J}^s_{ij}$ of eq. 1 we refer the reader to Ref. 25.) For the smaller field of 3.89 V/nm we obtain $D = 0.101$ meV nm per formula unit (f.u.), while doubling the field strength leads to $D = 0.195$ meV nm / f.u., i.e. the DMI grows almost linear with the field. Although the strength of the induced DMI is not sufficient to change the magnetic ground state of the film, in combination with the small spin stiffness and anisotropy this dependence indicate the possibility of the formation of metastable states like skyrmions. Finally, we want to mention that the major contribution to the DMI in this compound comes from the Bi atoms as the effect of the inner Te and surface Te almost cancel each other.

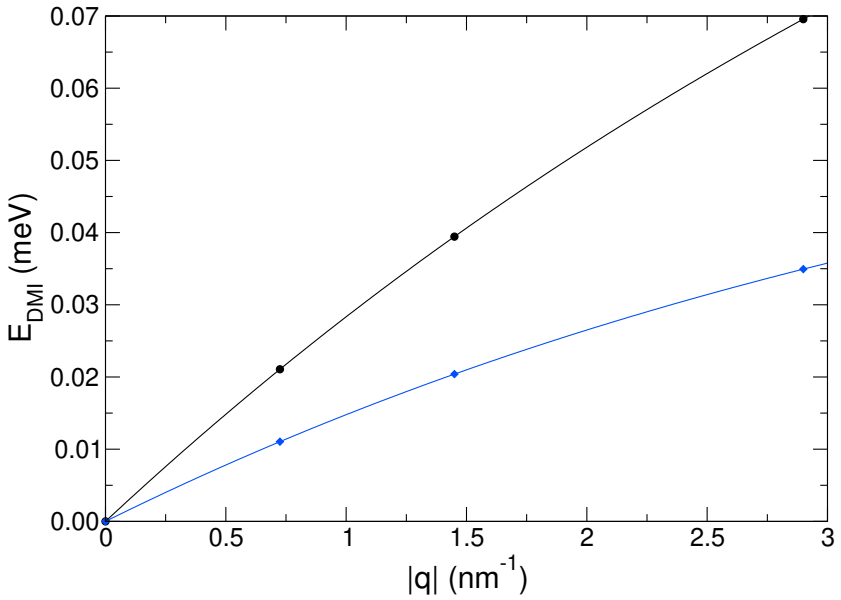

Figure 3. SOC induced variation of the total energy of long wave-length spin-spirals in $MnBi_2Te_4$ exposed to an electric field of 3.89 V/nm (blue diamonds) and 7.79 V/nm (black circles). The **q**-vector points in $\overline{\Gamma K}$ direction. Lines are cubic fits to the data points.

4. SUMMARY

We analyzed the exchange interactions in septuple layers of $MnBi_2Te_4$ type and found that the Heisenberg-type interactions are dominated by the nearest-neighbor term J_1, followed in importance by the biquadratic interaction $\mathcal{B}_1$. Important for the stability of long range order at finite temperatures are anisotropic interactions. Here the magnetocystalline anisotropy favors an easy axis magnetization (out-of-plane), but for $MnBi_2Se_4$ this is almost compensated – for $MnSb_2Te_4$ even overcome – by the dipole-dipole contribution to the magnetic anisotropy. Anisotropic exchange interactions give a small but significant contribution to the Curie temperature. Finally, although the DMI is zero for a freestanding septuple layer of these compounds, symmetry breaking by an electric field (or by embedding the layer in an asymmetric stack) leads to sizable antisymmetric exchange interactions in $MnBi_2Te_4$.

Compared with traditional metallic magnets, where often a few types of magnetic interactions are sufficient to describe the system, here a wide variety of contributions can be identified that is of relevance – maybe not so much for the ground state, but for metastable or excited states. We hope that this analysis sharpens the awareness for more exotic contributions of this kind in the studies of two-dimensional magnetic materials.

ACKNOWLEDGMENTS

We gratefully acknowledge computing time at the JURECA supercomputer from the Jülich Supercomputing Centre.

REFERENCES

[1] Novoselov, K. S., Mishchenko, A., Carvalho, A., and Castro Neto, A. H., "2D materials and van der Waals heterostructures," *Science* **353**(6298) (2016).

[2] Gong, C., Li, L., Li, Z., Ji, H., Stern, A., Xia, Y., Cao, T., Bao, W., Wang, C., Wang, Y., Qiu, Z. Q., Cava, R. J., Louie, S. G., Xia, J., and Zhang, X., "Discovery of intrinsic ferromagnetism in two-dimensional van der Waals crystals," *Nature* **546**, 265 (2017).

[3] Huang, B., Clark, G., Navarro-Moratalla, E., Klein, D. R., Cheng, R., Seyler, K. L., Zhong, D., Schmidgall, E., McGuire, M. A., Cobden, D. H., Yao, W., Xiao, D., Jarillo-Herrero, P., and Xu, X., "Layer-dependent ferromagnetism in a van der Waals crystal down to the monolayer limit," *Nature* **546**, 270 (2017).

[4] Deng, Y., Yu, Y., Song, Y., Zhang, J., Wang, N. Z., Sun, Z., Yi, Y., Wu, Y. Z., Wu, S., Zhu, J., Wang, J., Chen, X. H., and Zhang, Y., "Gate-tunable room-temperature ferromagnetism in two-dimensional Fe_3GeTe_2," *Nature* **563**, 94 (2018).

[5] Bonilla, M., Kolekar, S., Ma, Y., Diaz, H. C., Kalappattil, V., Das, R., Eggers, T., Guttierrez, H. R., Phan, M.-H., and Batzill, M., "Strong room-temperature ferromagnetism in VSe_2 monolayers on van der Waals substrates," *Nature Nanotech.* **13**, 289 (2018).

[6] Otrokov, M. M., Menshchikova, T. V., Vergniory, M. G., Rusinov, I. P., Vyazovskaya, A. Y., Koroteev, Y. M., Bihlmayer, G., Ernst, A., Echenique, P. M., Arnau, A., and Chulkov, E. V., "Highly-ordered wide bandgap materials for quantized anomalous Hall and magnetoelectric effects," *2D Materials* **4**, 025082 (2017).

[7] Otrokov, M. M., Rusinov, I. P., Blanco-Rey, M., Hoffmann, M., Vyazovskaya, A. Y., Eremeev, S. V., Ernst, A., Echenique, P. M., Arnau, A., and Chulkov, E. V., "Unique thickness-dependent properties of the van der Waals interlayer antiferromagnet $MnBi_2Te_4$ films," *Physical Review Letters* **122**(10), 107202 (2019).

[8] Li, Y., Jiang, Z., Li, J., Xu, S., and Duan, W., "Magnetic anisotropy of the two-dimensional ferromagnetic insulator $MnBi_2Te_4$," *Phys. Rev. B* **100**, 134438 (2019).

[9] Perdew, J. P., Burke, K., and Ernzerhof, M., "Generalized gradient approximation made simple," *Phys. Rev. Lett.* **77**(18), 3865–3868 (1996).

[10] Krakauer, H., Posternak, M., and Freeman, A. J., "Linearized augmented plane-wave method for the electronic band structure of thin films," *Phys. Rev. B* **19**(4), 1706–1719 (1979).

[11] Kurz, P., Förster, F., Nordström, L., Bihlmayer, G., and Blügel, S., "*Ab initio* treatment of non-collinear magnets with the full-potential linearized augmented planewave method," *Phys. Rev. B* **69**, 024415 (2004).

[12] Eremeev, S., Otrokov, M., and Chulkov, E. V., "Competing rhombohedral and monoclinic crystal structures in $MnPn_2Ch_4$ compounds: An ab-initio study," *Journal of Alloys and Compounds* **709**, 172–178 (2017).

[13] Herring, C., [*Exchange interactions among intinerant electrons, Magnetism Vol. IV*], ed. G. T. Rado, H. Suhl, Academic Press, New York, London (1966).

[14] Heide, M., Bihlmayer, G., and Blügel, S., "Describing Dzyaloshinskii-Moriya spirals from first principles," *Physica B* **404**, 2678 (2009).

[15] Ležaić, M., Mavropoulos, P., Bihlmayer, G., and Blügel, S., "Exchange interactions and local-moment fluctuation corrections in ferromagnets at finite temperatures based on noncollinear density-functional calculations," *Phys. Rev. B* **88**, 134403 (2013).

[16] Li, J., Ni, J. Y., Li, X. Y., Koo, H.-J., Whangbo, M.-H., Feng, J. S., and Xiang, H. J., "Intralayer ferromagnetism between $s = \frac{5}{2}$ ions in $MnBi_2Te_4$: Role of empty Bi p states," *Phys. Rev. B* **101**, 201408 (2020).

[17] Hoffmann, M. and Blügel, S., "Systematic derivation of realistic spin models for beyond-Heisenberg solids," *Phys. Rev. B* **101**, 024418 (2020).

[18] Krönlein, A., Schmitt, M., Hoffmann, M., Kemmer, J., Seubert, N., Vogt, M., Küspert, J., Böhme, M., Alonazi, B., Kügel, J., Albrithen, H. A., Bode, M., Bihlmayer, G., and Blügel, S., "Magnetic ground state stabilized by three-site interactions: Fe/Rh(111)," *Phys. Rev. Lett.* **120**, 207202 (2018).

[19] Yosida, K., "Theory of magnetism," in [*Springer Series in Solid-State Sciences, Vol. 122*], Cardona, M., Fulde, P., v. Klitzing, K., Merlin, R., Queisser, H. J., and Störmer, H., eds., Springer, Heidelberg (1996).

[20] Kurz, P., Bihlmayer, G., Hirai, K., and Blügel, S., "Three-dimensional spin structure on a two-dimensional lattice: Mn/Cu(111)," *Phys. Rev. Lett.* **86**, 1106–1109 (2001).

[21] Spethmann, J., Meyer, S., von Bergmann, K., Wiesendanger, R., Heinze, S., and Kubetzka, A., "Discovery of magnetic single- and triple-**q** states in Mn/Re(0001)," *Phys. Rev. Lett.* **124**, 227203 (2020).

[22] Al-Zubi, A., Bihlmayer, G., and Blügel, S., "Modeling magnetism of hexagonal Fe monolayers on 4d substrates," *physica status solidi (b)* **248**(10), 2242–2247 (2011).

[23] Bornemann, S., Minar, J., Braun, J., Koedderitzsch, D., and Ebert, H., "Ab-initio description of the magnetic shape anisotropy due to the Breit interaction," *Solid State Communications* **152**, 85–89 (2010).

[24] Torelli, D., Thygesen, K. S., and Olsen, T., "High throughput computational screening for 2D ferromagnetic materials: the critical role of anisotropy and local correlations," *2D Materials* **6**, 045018 (2019).

[25] Schweflinghaus, B., Zimmermann, B., Heide, M., Bihlmayer, G., and Blügel, S., "Role of Dzyaloshinskii-Moriya interaction for magnetism in transition-metal chains at Pt step edges," *Phys. Rev. B* **94**, 024403 (2016).